Adv Exp Med Biol - Cell Biology and Translational Medicine (2023) 19: 97–113
https://doi.org/10.1007/5584_2022_755

Published online: 10 December 2022

Leveraging Tissue Engineering for Skin Cancer Models

Sumayah Oudda, Abdulla M. Ali, Anna L. Chien, and Seungman Park

Abstract

Bioengineered in vitro three-dimensional (3D) skin model has emerged as a promising tool for recapitulating different types of skin cancer and performing pre-clinical tests. However, a full-thickness 3D model including the epidermis, dermis, and hypodermis layers is scarce despite its significance in human physiology and diverse biological processes. In this book chapter, an attempt has been made to summarize various skin cancer models, including utilized skin layers, materials, cell lines, specific treatments, and fabrication techniques for three types of skin cancer: melanoma, basal cell carcinoma (BCC), and squamous cell carcinoma (SCC). Subsequently, current limitations and future directions of skin cancer models are discussed. The knowledge of the current status of skin cancer models can provide various potential applications in cancer research and thus a more effective way for cancer treatment.

Keywords

Basal cell carcinoma (BCC) · In vitro 3D model · Melanoma · Skin cancer · Squamous cell carcinoma (SCC)

Abbreviations

5-FU	5-Fluorouracil
AK	Actinic Keratosis
ALA	Aminolevulinic Acid
BCC	Basal Cell Carcinoma
BEC	Blood Endothelial Cells
BLM	BRO Lung Metastasis
BM	Basement Membrane
CD31	Cluster of Differentiation 31
cDC2	Type-2 Conventional Dendritic Cells
Cldn4	Claudin 4
CLEC2A	C-Type Lectin Domain Family 2 Member A
cSCC	Cutaneous Squamous Cell Carcinoma
DED	De-Epidermized Dermis
ECM	Extracellular Matrix
EGF	Epidermal Growth Factor
EGFR	Epidermal Growth Factor Receptor

S. Oudda
Department of Biology, Johns Hopkins University, Baltimore, MD, USA

A. M. Ali
The Thomas C. Jenkins Department of Biophysics, Johns Hopkins University, Baltimore, MD, USA

A. L. Chien
Department of Dermatology, Johns Hopkins University School of Medicine, Baltimore, MD, USA

S. Park (✉)
Department of Mechanical Engineering, University of Nevada, Las Vegas, Las Vegas, NV, USA
e-mail: seungman.park@unlv.edu

G-CSF	Granulocyte Colony-Stimulating Factor
GFP	Green Fluorescent Protein
GM-CSF	Granulocyte-Macrophage Colony-Stimulating Factor
HBL	Human Diffuse Large B-cell Lymphoma
HGF/SF	Hepatocyte Growth Factor/Scatter Factor
HMVEC	Human Microvascular Endothelial Cells
HNSCC	Head and Neck Squamous Cell Carcinoma
HPV	Human Papillomavirus
LEC	Lymphatic Endothelial Cells
LEF-1	Lymphoid Enhancer Binding Factor 1
LOX	Lysyl Oxidase
MAPK	Mitogen-Activated Protein Kinase Pathway
MMP-9	Matrix Metalloproteinase-9
NBCSS	Nevoid Basal Cell Carcinoma Syndrome
NK	Natural Killer
OMA1	Overlapping with the m-AAA Protease 1 Homolog
PDPN	Podoplanin
Ptch1	Patched 1
RDEB	Recessive Dystrophic Epidermolysis Bullosa
RGP	Radial Growth Phase
RNAi	RNA Interference
SCC	Squamous Cell Carcinoma
SHH	Sonic Hedge Hog
SMO	Smoothened
TGFβ	Transforming Growth Factor Beta
TJ	Tight Junction
TNF- α	Tumor Necrosis Factor Alpha
TRAIL	Tumor Necrosis Factor-Related Apoptosis-Inducing Ligand
UV	Ultraviolet
VGP	Vertical Growth Phase

1 Introduction

Skin is commonly described as a protective layer because it is the body's first line of defense against many harmful threats. Over the past century, the increased exposure time to sunlight and UV has drastically increased the incidence of skin cancer (Zarebkohan et al. 2020). In the United States, skin cancer occurs in 5.4 out of every million (Cakir et al. 2012). Skin cancer is classified into three types: melanoma, basal cell carcinoma (BCC), and squamous cell carcinoma (SCC) (Fig. 1). Melanoma is the most dangerous cancer and accounts for 74% of the death toll, even though it makes up only 4% of all skin cancer cases (Dubas and Ingraffea 2013). Non-melanoma cancers, including SCC and BCC, are known to be less fatal than melanoma cancer, taking up 80% and 20%, respectively (Zarebkohan et al. 2020).

Various skin models have been utilized to better understand the molecular and cellular mechanisms involved in the development of cancer and to develop potential therapeutic methods for its treatment. A two-dimensional (2D) cell culture is one of the most common models for skin cancer research as well as many biological studies (Jensen and Teng 2020). However, numerous studies have revealed that there are considerable disparities between 2D and 3D tumor environments in terms of physiology, gene and protein profiles, cell/tissue function, and abnormal reaction toxicants (Carvalho et al. 2015; Duval et al. 2017; Lelièvre et al. 2017). For example, skin fibroblasts in 3D were physiologically relevant, having a dendritic shape, as opposed to in 2D, where they have a higher spreading area and more stress fibers (Park et al. 2015). As such, traditional 2D models have a very low translational potential. To reduce the gap between 2D and 3D in vitro models, animal models have been adopted due to their increased similarity to humans. Murine models were successfully tested to predict the efficacy and pharmacodynamics of anti-cancer drugs (Kuzu et al. 2015). However, there are still some limitations to animal models due to the inherent differences and a very low rate of reproducibility between humans and mice, thus resulting in less than 10% of data which is possible to translate (Carvalho et al. 2018; Mak et al. 2014). In the case of skin tissue, there was a significant difference in the architecture of the hypodermis between the two species

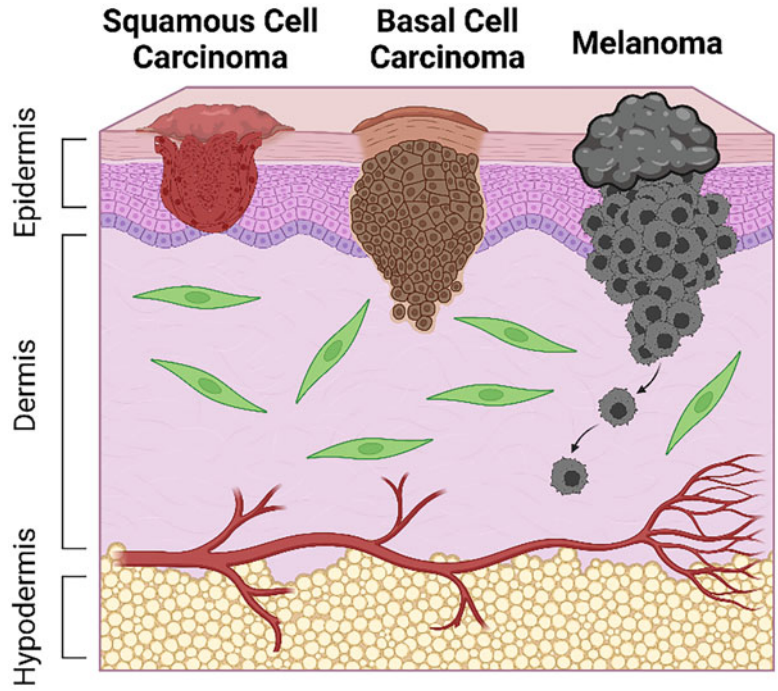

Fig. 1 Types of skin cancer. Squamous cell carcinoma (SCC) starts in the squamous cells of the skin, whereas basal cell carcinoma (BCC) develops in the basal cells. Melanoma, the deadliest form of skin cancer, frequently grows in a mole or is suddenly created as a dark spot, developing from melanocytes

(Khavari 2006). Hence, there is a necessity to develop a more effective system that mimics human physiology (Unnikrishnan et al. 2021).

Recent developments in 3D in vitro cancer models have provided an alternative to traditional approaches to recapitulate the tumor microenvironment with accuracy in a low-cost and simple manner (Li et al. 2019). The most commonly used methods for replicating 3D tumors include in vitro spheroids, microfluidics, assembling, tumor formation in 3D gels, and bioprinting (Asghar et al. 2015; Cui et al. 2017). These 3D in vitro models are more physiologically relevant, but data for studying skin cancer using these models are still scarce. Moreover, most of the 3D skin disease models, including cancer or wound healing, have utilized single- or double-layered tissues composed of epidermis or epidermis/dermis layers, excluding the hypodermis layer, despite its significance in several biological processes (Zimoch et al. 2021). In this review, we summarize various skin tissue models and their applications for cancer research using three different types of cancer: melanoma, SCC, and BCC. Since there are only a few studies using tri-layered skin tissue for skin cancer research in 3D in vitro models, we discuss the future directions regarding the role of adipose tissue in 3D skin cancer research.

2 Skin Cancer Models

2.1 Melanoma Skin Model

Melanoma is the deadliest skin cancer because of its apparent propensity to metastasize despite being the least frequent (Bourland et al. 2018). To mimic the melanoma microenvironment and understand the dynamics of melanoma cancer cells, diverse 2D and 3D melanoma skin models have been developed and utilized (Table 1).

A de-epidermized skin tissue model has been widely used for melanoma research. An organotypic skin melanoma construct consisting of a stratified epidermis, basement membrane, and dermis was fabricated by utilizing a de-epidermized, de-cellularized dermis (DED)

Table 1 Studies using melanoma skin tissue models

Skin layer	Material	Cell type	Fabrication method	Signaling molecule/ protein	Additional component	Reference
Epidermis Basement membrane Dermis	Rat tail collagen type I	Keratinocytes Fibroblasts 451-LU (metastatic melanoma cells)	Manual Hanging drops	Epidermal growth factor	TRAIL (tumor necrosis factor-related apoptosis-inducing ligand) UVB Cisplatin	Vörsmann et al. (2013)
Epidermis Basement membrane Dermis	De-epidermized dermis	Keratinocytes Fibroblasts WM35 (melanoma cell line- radial growth phase) SK-MEL-28 (melanoma cell line-metastatic phase)	Manual			Haridas et al. (2017)
Epidermis Basement membrane Dermis	Rat tail collagen type I	Keratinocytes Fibroblasts Melanocytes WM35 (RGP melanoma cells) WM793 and WM115 (VGP melanoma cells) WM852 (metastatic melanoma cells)	Manual	EGF bFGF/Ad5		Meier et al. (2000)
Epidermis Basement membrane Dermis	Rat tail collagen type I	Keratinocytes Fibroblasts Melanoma cells	Manual		PLX4032 (Vemurafenib)	Lee et al. (2010)
Dermis	Rat tail collagen type I	Fibroblasts 451Lu and SKMel28 melanoma cells	Manual		RAF kinase inhibitor MEK inhibitors PI3K inhibitors	Meier et al. (2007)
Epidermis Basement membrane Dermis	De-epidermized dermis 0.5% collagenase A solution	Keratinocytes Fibroblasts HBL melanoma cells A375-SM melanoma cells C8161 melanoma cells	Manual	TNF-alpha Fibrin clot solution	Fibrin Ibuprofen	Marques and MacNeil (2016)
Epidermis Basement membrane Dermis (without stromal fibroblasts)	De-epidermized dermis	Keratinocytes Adherent melanoma cells (BLM)	Manual	Epidermal growth factor		Van Kilsdonk et al. (2010)
Epidermis Basement membrane Dermis	Collagen matrix	Keratinocytes Fibroblasts A375 melanoma cell line 451Lu melanoma cell line	Model produced by MatTek		Fisetin	Syed et al. (2014)

(continued)

Table 1 (continued)

Skin layer	Material	Cell type	Fabrication method	Signaling molecule/ protein	Additional component	Reference
Epidermis Basement membrane Dermis	Anchor papers	Keratinocytes Fibroblasts Human microvascular endothelial cells (HMVEC: includes blood and lymphatic endothelial cells) A375, Malme 3 M, SK-MEL 28, RPMI 7951, WM983A, and WM983B melanoma cells	Self-assembly method Hanging drops	Epidermal growth factor	Vermurafenib	Bourland et al. (2018)
Epidermis Basement membrane Dermis	De-epidermized dermis	Keratinocytes Fibroblasts BLM, BLM-GFP, Mel624, and A375 melanoma cells cDC2s	Manual Microneedle array system	Epidermal growth factor Keratinocyte growth factor		Di Blasio et al. (2020)

(Di Blasio et al. 2020). Fibroblasts were seeded onto the reticular dermal side of the DED while keratinocytes were later seeded onto the papillary side, on top of the basement membrane. Various melanoma cell lines including BLM, BLM-GFP, Mel624, and A375 were incorporated into the epidermis and dermis. To assess the impact of tumor microenvironment on immune cells, type-2 conventional dendritic cells (cDC2s) were then seeded into the dermis. The 3D skin model in this study demonstrated that the tumor microenvironment transforms wildtype, immunostimulatory cDC2s into immunosuppressive CD14+ dendritic cells that cannot effectively induce T-cell activation. This model highlights one manner in which melanoma cells propagate changes that weaken the immune system.

Kilsdonk et al., similar to the previous study (Di Blasio et al. 2020), also used a de-epidermized dermis to construct an organotypic skin model (Van Kilsdonk et al. 2010). The DED contained the de-cellularized dermal component and the basement membrane (BM), which were taken advantage of by carrying out trials where melanoma cells were either seeded into the reticular dermis or on top of the basement membrane, without keratinocytes included at first. In addition, no fibroblasts were incorporated into the skin construct in order to focus on the cell interactions between melanoma and keratinocytes. When metastatic melanoma cells (BLMs) were seeded onto the basement membrane without keratinocytes, the BM served as a barrier for invasion, and the melanoma cells could not cross into the dermis. In contrast, when keratinocytes were incorporated to form a stratified epidermis conjoined with the dermis, BLM invasion occurred. The experiments supported evidence that cross-talk between keratinocytes and metastatic melanoma cells is required for encouraging BLMs to pass through the BM by activating proteases such as MMP-9.

Marques et al. also utilized a de-epidermized dermis where fibroblasts were seeded onto the reticular dermis, and keratinocytes and melanoma cells were seeded onto the papillary surface (Marques and MacNeil 2016). This study was motivated by the fact that patients experience a local recurrence of melanoma in the wound bed post-surgical excision of the primary tumor. The 3D skin tissue model, complete with a stratified epidermis, basement membrane, and dermis, received a wound by using a scalpel blade to form a cut through the epidermis and into the dermis. The in vitro model demonstrated that inflammation can heighten melanoma invasion but be reduced by anti-inflammatory treatment

using three different melanoma cell lines: A375SM and HBL invasion were increased by wounding and decreased with ibuprofen treatment, while C8161's severe invasion was not impacted by wounding, TNF-α, or ibuprofen. The 3D skin tissue model used in this study has proved to be an immensely useful tool for assessing the behavior of different melanoma cell lines' unique responses to external factors.

Two different melanoma cell lines – WM35 and SK-MEL-28 – were employed to study cell invasion using a 3D skin equivalent model consisting of de-epidermized dermis containing fibroblasts, keratinocytes, and melanoma cells (Haridas et al. 2017). The invasion of the melanoma cell lines was quantified over 3 weeks, and the results demonstrated that SK-MEL-28 melanoma cells invaded the dermis quickly; at a slower rate, WM35 melanoma cells eventually invaded the dermis as well. In addition, as the invasion progressed, the basement membrane lost integrity, being partially absent. This led to the conclusion that interference with the basement membrane is potentially associated with the transition from the radial growth phase (RGP) to the vertical growth phase (VGP).

Lee et al. fabricated a human skin equivalent with a stratified epidermis, basement membrane, and dermis by means of the manual method (Lee et al. 2010). An acellular collagen foundation was set first, followed by a mixture of fibroblasts with rat tail collagen placed on top. Finally, keratinocytes and melanoma cells were seeded last. An inhibitor of BRAF V600E, PLX4032 (vemurafenib), an established drug used in melanoma treatment, was then applied to the skin construct. Results showed that PLX4032 exclusively decreased proliferation and induced apoptosis of melanoma cells with the BRAF V600E mutation. Furthermore, the tumors were diminished, highlighting the aggressive impact of the inhibitor on melanoma cells with the V600E oncogene.

The self-assembly method was leveraged to fabricate an organotypic skin melanoma substitute with a stratified epidermis, basement membrane, dermis, blood vessels, and lymphatic vessels (Bourland et al. 2018). This model, which highly mimics native skin, involved seeding fibroblasts onto three anchor papers to form cell sheets. Human microvascular endothelial cells (HMVEC) including lymphatic endothelial cells (LEC) and blood endothelial cells (BEC) were seeded into two of the cell sheets. On the third cell sheet, melanoma spheroids and keratinocytes were seeded. The three cell sheets were at last layered together to form the human skin substitute. The study exhibited that blood and lymphatic vessels were successfully formulated, distinguished by markers such as CD31 and PDPN; the vessels were also metabolically active, as seen by an increased presence of chemokine ligand 21 and angiopoietin-2. By including capillary networks, the 3D model more accurately represents native skin compared to 2D and 3D models without endothelial cells. The substitute was also assessed when treated with vemurafenib, and results showed that the proliferation of melanoma cells decreased significantly after treatment, although some proliferative cancer cells remained.

Syed et al. utilized a full-thickness skin model with A375 melanoma cells that are commercially produced by MatTek Corporation (Syed et al. 2014). The model includes a differentiated epidermis and dermis alongside the melanoma cells exhibiting RGP, VGP, and metastatic behavior. It should be noted that the in vitro skin equivalent was supplemented with media, both with and without fisetin (i.e., control), a tetrahydroxyfalvone. Results revealed that the fisetin-treated samples had significantly reduced melanoma cells and melanocytic lesions compared to the control. The study also highlighted that the experimental treatment did not cause any notable damage to the keratinocytes or fibroblasts, thus showcasing the advantage of using 3D skin constructs to assess not only the effects of potential drug treatments on melanoma but also on the skin morphology as a whole. Further investigation discovered that fisetin directly interacts with and binds to mTOR and p70S6K, suggesting that fisetin's antiproliferative effect stems from its interference in cell-signaling pathways.

A simple single- or double-layered skin model has also been widely used. A skin equivalent comprised of only the dermis, no basement

membrane nor epidermis present, was constructed using an acellular collagen solution made from rat tail collagen type I (Meier et al. 2007). A collagen matrix with fibroblasts and metastatic melanoma cells (with the V600E mutation) was then placed over the acellular layer. When the matrix was treated with the media containing MEK inhibitors, PI3K inhibitors, and/or RAF kinase inhibitor, the fibroblasts were not impacted by treatment. However, the RAF kinase inhibitor and the PI3K inhibitor, when used individually, decreased the melanoma invasion throughout the dermis. Moreover, using the two types of inhibitors together resulted in complete tumor suppression with only few melanoma cells left in the construct. This study demonstrates the opportunity to use bioengineered skin tissue for pre-clinical, in vitro testing of potential treatments that target cell signaling pathways such as MAPK and AKT. In another study, Meier et al. constructed double-layered skin mimetic tissue using the manual method, producing a stratified epidermis, basement membrane, and dermis. Similarly, a fibroblast-collagen matrix was set onto the acellular foundation and supplemented with medium containing epidermal growth factor. Subsequently, keratinocytes and melanoma cells were seeded. Results showed that basement membrane was successfully synthesized in vitro by fibroblasts and keratinocytes in the skin equivalent. Furthermore, transduction of the bFGF gene into melanoma cells exhibiting radial growth phase (RGP) allowed RGP melanoma cells to invade and nest in the dermis, a characteristic not seen without transduction. This model represents a potential application to study individual genes and their influence on melanoma phenotypes.

2D and 3D melanoma models were tested and compared to explore the effects of a chemotherapy drug and UVB using organotypic skin tissue, including a stratified epidermis, basement membrane, and dermis (Vörsmann et al. 2013). Melanoma spheroids, made of the metastatic 451-LU cell line, were produced by placing the cells using the hanging drop method and were embedded into the fibroblast-collagen matrix. The spheroids were treated with tumor necrosis factor-related apoptosis-inducing ligand (TRAIL) and ultraviolet-B radiation (UVB), whereas others were treated with TRAIL and cisplatin. The study observed that whereas 2D melanoma models showed tumor cell death for TRAIL +UVB and TRAIL+cisplatin, only the latter caused apoptosis in melanoma spheroids of the 3D skin construct. Thus, UVB lost its ability to render melanoma tumors sensitive to TRAIL once the tumors were in the heterogenous model that better represented native skin. Furthermore, the TRAIL+cisplatin treatment selectively targeted melanoma cells since apoptosis was not induced in fibroblasts or keratinocytes. Overall, this study underscores that 2D results do not necessarily translate to 3D outcomes, reiterating the need to use multilayered 3D skin constructs for pre-clinical research.

2.2 Squamous Cell Carcinoma (SCC) Skin Model

Squamous cell carcinoma (SCC), the second most prevalent type of skin cancer, is characterized by aberrant, accelerated squamous cell proliferation. Similar to the melanoma model, single- or double-layered skin tissues have been commonly available using diverse fabrication methods, including a cutting-edge bioprinting technique (Table 2).

Browning et al. adopted a 3D skin model through a bioprinting method detailed by Derr et al. (Derr et al. 2019), to study cutaneous squamous cell carcinoma, where the model is composed of a stratified epidermis, basement membrane, and dermis (Browning et al. 2020). A commercial bioprinter (REGENHU 3D Discovery Bioprinter) was used to fabricate the dermis. In brief, fibroblasts were loaded into a syringe that was loaded into the bioprinter and then dispensed into the hydrogel consisting of gelatin, fibrinogen stock solution, collagen I, and elastin. A laminin/entactin solution was then hand-pipetted onto the dermal foundation to form the basal layer, followed by the deposition of keratinocytes. Afterward, A431 cSCC spheroids were manually placed onto the top of the skin

Table 2 Studies using SCC skin tissue models

Skin layer	Material	Cell type	Fabrication method	Additional component	Reference
Epidermis Dermis Basement membrane	Gelatin Fibrinogen stock solution Collagen I Elastin Laminin/ entactin	Keratinocytes Fibroblasts A431 cSCC cells	Bioprinting	RegenHU 3DDiscovery bioprinter	Browning et al. (2020)
Epidermis Dermis Basement membrane	Collagen G (collagen I and III)	Keratinocytes Fibroblasts SCC 12 cells	Manual	δ-Aminolevulinic acid (ALA, photosensitizer drug) Visible radiation (545 nm)	Obrigkeit et al. (2009)
Epidermis Dermis Basement membrane	Rat tail collagen I Fibronectin solution	Keratinocytes Fibroblasts SCC-25 cells	Manual		Brauchle et al. (2013)
Epidermis Dermis Basement membrane	Collagen I	Keratinocytes Fibroblasts SCC-12 cells	Manual	Ingenol mebutate gel	Zoschke et al. (2016)
Epidermis Dermis	Collagen I	Fibroblasts SCC12 cells Natural killer cells	Manual	Anti-CLEC2A blocking antibody OMA1	Gonçalves-Maia et al. (2020)
Epidermis Dermis	Rat collagen I	Fibroblasts HNO97, HNO199, HNO136, HNO206 (head and neck squamous cell carcinoma cells)	Manual	G-CSF and GM-CSF antibody against G-CSF and GM-CSF	Gutschalk et al. (2006)
Epidermis Dermis	Rat tail collagen I Matrigel	RDEB fibroblasts RDEB-cSCC keratinocytes (recessive dystrophic epidermolysis bullosa)	Manual	SB505124 PF573228 β-aminopropionitrile LY294002	Mittapalli et al. (2016)
Epidermis Dermis	Viscose fiber fabric	Fibroblasts Head and neck squamous cell carcinoma tissue slices	Manual	Fractionated irradiation	Engelmann et al. (2020)
Epidermis		Ker-CT (keratinocyte cell line)	Manual		Smirnov et al. (2019)
Epidermis Basement membrane Dermis	De-epidermized dermis	Fibroblasts Keratinocytes with recombinant retroviruses	Manual	pLXSN-8E7 retrovirus	Akgül et al. (2005)

model. It was observed that the cSCC cells exhibited radial and vertical growth phase. In addition, the model's integrity was supported by gene expression analysis that agreed with findings from in vivo cSCC studies. Certain groups were treated with 5-fluorouracil (5-FU), a chemotherapeutic drug, and results demonstrated that 5-FU selectively killed cSCC cells with insignificant toxicity to the non-cancerous keratinocytes.

An organotypic skin that consisted of a stratified epidermis, basement membrane, and dermis was created by means of the manual method to study photodynamic therapy, which involves a photosensitizer and light (Obrigkeit et al. 2009). Collagen III as well as Collagen I-containing fibroblasts served as the dermal component, and keratinocytes were seeded onto the dermal layer, followed by SCC 12 cells that were placed onto

the center of the construct. Experimental observations revealed that the cancerous cells in the skin equivalent exhibited characteristics similar to in vivo studies such as irregularly shaped keratinocytes with larger nuclei and the ability to proliferate in the epidermis and eventually the dermis. In addition, the photodynamic experiments consisted of a control group, a group treated solely with a pro-photosensitizer, a group treated with green light, and a group treated with both pro-photosensitizer and green light. The pro-photosensitizer, δ-aminolevulinic acid (ALA), converts to the photosensitizer protoporphyrin when placed in the tissue environment. Only in the experimental group treated with both ALA and green light was there substantial impact: SCC tumor size decreased, SCC apoptosis was induced, and SCC mitotic activity decreased. Since photodynamic therapy had already been integrated as a treatment for patients with SCC prior to these experiments, this research helped validate the use of SCC skin equivalents to reliably study the effects of potential cancer-targeting drugs.

A 3D SCC skin model consisting of a stratified epidermis, basement membrane, and dermis was used to understand the characteristics of SCC cells (Brauchle et al. 2013). Fibroblasts were embedded in rat tail collagen I and fibronectin solution was placed onto the collagen matrix. Then, either keratinocytes or SCC-25 cells were seeded onto the dermal component for a non-cancerous or SCC cancerous model, respectively. The disease model did not exhibit robust spatial organization nor a stratified corneous layer in contrast to the non-cancerous model. The SCC model illustrated characteristics similar to in vivo studies: keratin accumulations were present, and capsular tumor cell nests were formed. Unlike in vivo experiments, SCC-25 cells had not infiltrated the dermis spontaneously. This study also found that SCC-25 cells appeared to have weak cell-cell contacts, as seen by small gaps between the cells in the epidermis. Uniquely, Raman spectroscopy, a non-invasive technique, was utilized to distinguish between non-cancerous and cancerous models using differences in the Raman spectra. This form of spectroscopy proved useful in identifying SCC versus non-SCC skin tissue.

Zoschke et al. also used engineered human skin using the manual fabrication method that resulted in an organotypic model with a stratified epidermis, basement membrane, and dermis (Zoschke et al. 2016). Collagen I formed the foundation and was then layered with further collagen I integrated with fibroblasts. Keratinocytes were seeded onto the dermal layer, and the cancerous models added SCC-12 cells into the epidermis. SCC models were incorporated with different ratios of keratinocytes to SCC-12 cells to represent different stages of SCC (epidermal invasion only or epidermal and dermal invasion). Certain experimental groups received topical treatment of Ingenol mebutate gel, a drug that has been used for patients with non-melanoma skin cancer. Whereas non-cancerous models had a fully stratified epidermis, SCC models did not and were found to have parakeratosis. SCC-12 cells were also found to break down the basal membrane. The stratum spinosum of disease models had "architectural disarray". Thus, the organotypic models proved useful in assessing a layer-by-layer look at the effect of SCC on skin. In addition, proteins related to the tight junction (TJ) were assessed: in SCC models, certain TJ proteins were reduced, such as Cldn4 and occludin. Numerous other differences were described as well; the stratum corneum of cancer models had lower lipid to protein ratios, lower cholesterol and ceramide levels, and a greater excess in phospholipids than non-cancerous models. Organotypic samples with more invasive SCC had a higher surface pH than normal. To study the permeability of skin tissue, caffeine permeation was assessed, and the SCC epidermis-dermis model had a permeability coefficient more than two-fold of the non-cancerous model. Furthermore, certain experimental groups were treated topically with Ingenol mebutate gel, which resulted in epidermal cell necrosis in both non-cancerous and cancerous models, resembling the outcomes of actinic keratosis (AK) patients who received application of the drug and experienced pain and skin irritation. Overall, these findings suggest that SCC presence in the skin may result in impaired skin barrier function and that organotypic skin is a suitable method of studying topical treatments.

Natural killer (NK) cells were incorporated into organotypic skin tissue, including an epidermis and dermis (Gonçalves-Maia et al. 2020). The NK cells were embedded into a collagen I matrix; fibroblasts in collagen I, seeded above by SCC-12 cells, were then placed onto the NK cell layer. Experimental observation revealed that the NK cells were able to move upward into the dermal component. In addition, this study examined how the interaction between fibroblasts and NK cells through the expression of CLEC2A genes impacts SCC-12 progression. In organotypic models of wild-type fibroblasts that expressed CLEC2A, the immune cells decreased the invasion of SCC-12. However, in models with xeroderma pigmentosum fibroblasts or cancer-associated fibroblasts, both of which do not significantly express CLEC2A, the NK cells did not reduce the cancer's invasion rate. In experiments with wild-type fibroblasts treated with anti-CLEC2A blocking antibody OMA1, SCC-12 invasion was prominent as well. These studies highlight the significance of different cell types and their gene profile to understand how squamous cell carcinoma behaves.

Gutschalk et al. investigated the behavior of head and neck squamous cell carcinoma using a manually produced organotypic model with an epidermis and dermis (Gutschalk et al. 2006). Fibroblasts were combined with rat collagen type I to form the dermal equivalents and various head and neck squamous cell carcinoma (HNSCC) lines were seeded on top for different experimental purposes. Certain trials employed HNSCC cells that secreted granulocyte colony-stimulating factor (G-CSF) and granulocyte-macrophage colony-stimulating factor (GM-CSF). Addition of G-CSF and GM-CSF to cell lines, whether they already had the capacity to secrete them, increased migration and proliferation in the organotypic models. Cell lines that secrete G-CSF and GM-CSF themselves were characterized by invasion into the dermal equivalent; however, when antibodies to the two factors were incorporated, the tumor cells' invasive ability was severely reduced. The study highlighted the need to re-evaluate the potential side effects of using G-CSF and GM-CSF to treat certain secondary effects of cancer treatment.

Engelmann et al. studied the heterogeneous nature of head and neck squamous cell carcinoma (HNSCC) using organotypic skin models, including an epidermis, dermis, and immune cells as well (Engelmann et al. 2020). Rather than using a collagen-based scaffold, the dermal equivalent was created by culturing fibroblasts on a viscose fiber fabric, a technique that allows the fibroblasts to produce the extracellular matrix. To assess characteristics of cancer cell behavior at a patient-specific level, HNSCC samples from patients, which either came from HPV-driven HNSCC or non-HPV-driven HNSCC, were sliced, and the tissue slices were overlayed on top of the dermal equivalent. The organotypic models that utilized tissue samples of non-HPV driven HNSCC had similar morphology to the primary tumors of the patients they were derived from; meanwhile, there were notable deviations between HPV-derived models and their corresponding primary tumors, such as p16INK4a expression later in the trials. Models from different patients could also exhibit different proliferation behaviors: invasive growth pattern (growth into the dermis), expansive growth pattern (horizontal growth in the epidermis), and silent growth pattern (neither invasion nor expansion). Certain experimental groups were treated with fractionated irradiation, and the irradiation caused varying effects on the unique cancer models, mimicking how patients with SCC may respond differently to the same treatment. Overall, this study emphasizes the value of organotypic tissue as a fast and effective way to evaluate a variety of parameters and responses.

An in vitro skin disease model composed of two layers (epidermis and dermis) was utilized to study recessive dystrophic epidermolysis bullosa (RDEB) and associated cutaneous squamous cell carcinoma (cSCC) (Mittapalli et al. 2016). The disease model consisted of a matrix of rat tail collagen I, matrigel, and RDEB fibroblasts. cSCC keratinocytes obtained from RBED samples (RBED-cSCC keratinocytes) were seeded onto the dermal layer to form the epidermis. Inhibitors of TGFβ signaling, lysyl oxidase (LOX), or integrin β1-mediated mechanosignaling were added to the model's culture medium to

observe their effect toward cancerous invasion (inhibitors included SB505124, PF573228, β-aminopropionitrile, LY294002). Experimental models with RBED fibroblasts and RBED-cSCC keratinocytes had cancer cells invading the dermal equivalent, while models with normal human fibroblasts did not. Moreover, organotypic skin with RBED fibroblasts had significantly stiffer matrices than normal fibroblasts. When inhibitors such as SB505124 (TGFβ signaling) or β-aminopropionitrile (LOX inhibitor) were used as treatments, matrix stiffening and collagen fibril thickness decreased, respectively, which subsequently decreased the invasion of cancerous cells. This research underscored how cSCC is invigorated by the extracellular matrix conditions produced by RBED, bringing attention to the relationships between different skin diseases.

Akgül et al. utilized a de-epidermized dermis seeded with fibroblasts within the stroma and keratinocytes on top of the papillary side of the dermis to assess the effect of certain HPV oncogenes on keratinocytes (Akgül et al. 2005). In the disease models, keratinocytes were transduced with pLXSN-8E7 retrovirus, which causes the keratinocytes to produce the E7 protein of HPV type 8. It was observed that in the transduced models, keratinocytes invaded the dermis and horn pearls were formed; the basement membrane (BM) was also disrupted, and collagen VII, a marker of the BM, was reduced. Certain extracellular matrix (ECM) metalloproteinases were upregulated and likely caused the degradation of ECM components that were found to have normal levels in the control groups but decreased in experimental models. These findings highlight HPV's ability to induce the invasive keratinocyte phenotype seen in squamous cell carcinoma.

A 3D organotypic model only composed of the epidermis was used to study keratinocyte differentiation (Smirnov et al. 2019). Ker-CT cells from an immortalized keratinocyte cell line were manually seeded on inserts and placed on culture dishes. The samples were later exposed to air-lifting, and the stratified epidermis then underwent immunofluorescence analysis for ZNF185, a protein proven necessary for keratinocyte differentiation. The organotypic model had observable and abundant ZNF185. In contrast, experiments with RNAi-knockdown of p63, a transcription factor for ZNF185, demonstrated a significant decrease in ZNF185, which disrupted cell-cell adhesion and tissue stability. These results helped confirm that p63 had a direct impact on ZNF185 expression; genetic analysis revealed that p63 serves as a transcription factor that binds to an enhancer of ZNF185. Such results may imply that squamous cell carcinomas with inadequate keratinocytes differentiated could have a loss of ZNF185 expression or function.

2.3 Basal Cell Carcinoma (BCC) Skin Model

Compared to melanoma and SCC, BCC is generally less invasive and metastatic; BCC is thus incorporated into 2D in vitro studies more frequently than 3D organotypic models. Since BCC cells are not propagated ex vivo (Gache et al. 2015), most bioengineered organotypic models used to study BCC employ other keratinocyte cell types, often genetically altered, as seen in the research below (Table 3).

Bigelow et al. manually formulated a 3D organotypic BCC model consisting of a stratified epidermis, basement membrane, and dermis (Bigelow et al. 2005). Fibroblasts were integrated with collagen to serve as the dermal equivalent. HaCaT (human epidermal keratinocytes) cells were transfected with a vector containing shh cDNA, which codes for a protein (shh) active in a cell signaling pathway involved in the development of basal cell carcinoma called the sonic hedgehog (shh) pathway (Dahmane et al. 1997). The shh HaCaT cells were seeded onto the dermal equivalent to form the epidermal layer. Comparison between control HaCaT versus shh HaCaT experiments highlighted a few notable differences: keratinocytes in shh models maintained cuboidal morphology after stratification, whereas control keratinocytes had the expected squamoid shape in superficial layers; the shh model infiltrated the dermal layer, whereas the control did not; the shh model had upregulated matrix metalloproteinase

Table 3 Studies using BCC skin tissue models

Skin layer	Material	Cell type	Fabrication method	Signaling molecule/ protein	Additional component	Reference
Epidermis Basement membrane Dermis	Collagen	HaCaT cells (keratinocytes) transfected with Shh Fibroblasts	Manual	Recombinant EGF protein	Shh cDNA in Bill Neo Vector AG1478 (EGF inhibitor)	Bigelow et al. (2005)
Epidermis Basement membrane Dermis	Chitosan-cross-linked collagen-GAG matrix	Keratinocytes Fibroblasts HaCat cells (keratinocytes) transfected with LOX antisense constructs	Manual	Epidermal growth factor	pcDNA3 and LipofectAMINE (for transfection) β-aminoproprionitrile (inhibitor of LOX activity)	Bouez et al. (2006)
Epidermis Basement membrane Dermis	Type I collagen	Keratinocytes with PATCHED ± phenotype Fibroblasts	Manual			Brellier et al. (2008)
Epidermis Basement membrane Dermis	Matrigel Type I collagen	NTert-1 cells (keratinocytes) transfected with Gli1 or Gli2 Fibroblasts	Manual		pBabePuro and retroviral particles β6 RNAi SU11274 (MET kinase inhibitor)	Marsh et al. (2008)
Epidermis Basement membrane Dermis	Type I bovine collagen gel	Keratinocytes NBCCS (nevoid basal cell carcinoma syndrome) fibroblasts	Manual		Anti-SHH (Sonic hedgehog) 5E1 monoclonal antibody Isotype-matched anti-cMyc 9E10 monoclonal antibody	Gache et al. (2015)
Epidermis Basement membrane Dermis	Matrigel Collagen	Keratinocytes (HaCaT/NEB1/N/Tert) transfected with PTCH1 small hairpin RNA Fibroblasts	Manual		PTCH1 small hairpin RNA SMO RNAi	Rahman (2013)
Epidermal mimic	Laminin-rich extracellular matrix	BCC-1 cells	Manual		Vismodegib Radiation	Hehlgans et al. (2018)

and cytokeratin 14 in contrast to the control. Importantly, the shh model had higher levels of EGF (epidermal growth factor) receptor phosphorylation on serine 845 and 1068, increasing the EGFR signal propagation. When EGF was added to control and shh models, both sets of experiments demonstrated an increase of dermal infiltration relative to their non-EGF-treated counterparts (the control had no invasion prior to EGF addition). When an EGF signaling inhibitor was applied, dermal invasion of the shh model was decreased significantly. Overall, this research elucidated the presence of a shh-EGF signaling pathway relationship that resulted in the basal cell carcinoma phenotype (Bigelow et al. 2005).

Bouez et al. sought to study the importance of lysyl oxidase (LOX) in BCC as well as overall epidermal homeostasis and crafted an organotypic model consisting of a stratified epidermis, basement membrane, and dermis (Bouez et al. 2006). The model was generated manually, first by seeding fibroblasts into a chitosan-cross-linked collagen-GAG matrix to form the dermal equivalent. Then, either keratinocytes, wild-type

HaCaT cells, vehicle vector HaCaT cells, or HaCaT cells transfected with an antisense LOX construct were seeded on top of the dermal layer. Experimental models were treated with β-aminoproprionitrile, an inhibitor of LOX activity. Results showed that LOX was absent from tumor cells of BCC samples from patients but was notably present in the stroma surrounding the cancerous cells. In the organotypic models treated with β-aminoproprionitrile, collagen fibers appeared less regular in their size and shape. Furthermore, the lamina densa, a component of the basement membrane, was disorganized in the presence of the LOX activity inhibitor. β-Aminoproprionitrile was limited in that it did not promote invasion of the keratinocytes into the dermis. In striking contrast, the only experimental model that exhibited invasion into the dermis was the model incorporating HaCaT cells transfected with an antisense LOX construct. Thus, interruption of LOX's expression and not solely its recognized enzymatic activity was required to develop a BCC-infiltration phenotype, opening a line of question to what unknown functions or associations LOX may also have.

Brellier et al. crafted an organotypic skin model manually, using the protocol detailed by Bernerd et al.'s study of epidermal cancer (Bernerd et al. 2001; Brellier et al. 2008). Brellier et al.'s model involved a 3D construct with a stratified epidermis, basement membrane, and dermis. The dermal layer consisted of fibroblasts integrated with type I collagen; the epidermal layer for the experimental models consisted of keratinocytes from patients with a genetic syndrome called nevoid basal cell carcinoma which makes an individual more susceptible to BCC. The patient-derived keratinocytes had a genotype of PATCHED +/− whereas wild-type keratinocytes had a phenotype of PATCHED +/+. The PATCHED +/− model displayed invasion into the dermis, unlike the control. The experimental model also exhibited higher levels of laminin B1 and beta-1 integrin and lower levels of keratin 10 and loricrin. Importantly, the PATCHED +/− model demonstrated a notable increase in cyclin D1 (cell cycle regulator) compared to the control. Interestingly, the amount of PATCHED mRNA in the control and experimental groups were similar, so a discrepancy in PATCHED transcriptional expression did not explain the BCC-like phenotype of the heterozygous model (Brellier et al. 2008).

Marsh et al. similarly created a 3D skin model consisting of an epidermis, basement membrane, and dermis by seeding fibroblasts into a 50:50 matrix of Matrigel and type I collagen (Marsh et al. 2008). Keratinocytes retrovirally transfected with Gli1, a transcription factor associated with BCC development, were then seeded onto the dermal foundation. The research sought to uncover the impact of αvβ6 integrin toward BCC invasion since αvβ6 is overexpressed in a more aggressive subtype of BCC called morphoeic BCC. The Gli1-transfected keratinocytes did indeed express αvβ6. In transwell experiments devoid of fibroblasts, αvβ6 did not supplement the invasion of Gli1 keratinocytes. However, with the combination of results from transwell, co-culture, and organotypic experiments, the indirect relationship between αvβ6 and invasive BCC behavior was uncovered. αvβ6 activated TGF-β1 (transforming growth factor); TGF-β1 caused fibroblasts to transition into myofibroblasts; myofibroblasts increase HGF/SF (hepatocyte growth factor/scatter factor); HGF/SF signalizing promoted the infiltration of transfected keratinocytes. The organotypic skin assisted in understanding this sequence: in the 3D construct where β6 RNAi was included to suppress αvβ6 expression, the transfected keratinocytes had reduced invasion, assumingly because fibroblasts did not become myofibroblasts. In organotypic experiments where SU1224 (a Met kinase inhibitor) was used to disrupt the HGF/SF signaling pathway, reduced invasion was also observed.

Gache et al. developed an organotypic skin model to study dermal-epidermal interactions of nevoid basal cell carcinoma syndrome (NBCCS) (Gache et al. 2015). In the experimental groups, NBCCS fibroblasts were embedded in type I bovine collagen gel to form the dermal equivalent. Wild-type keratinocytes were then seeded onto the dermis. Certain experiments were treated with anti-SHH (Sonic Hedge Hog) 5E1 monoclonal antibody (while the control for this group was treated with the isotype-matched anti-cMyc 9E10

monoclonal antibody). The NBCCS-fibroblasts organotypic models resulted in an epidermis of lower thickness, loss of bona fide cornified layers, parakeratosis, increased deposition of LamininB1 and β1 Integrin, and clefts at the dermo-epidermal junction. Interestingly, the NBCCS models also demonstrated a substantial increase in p53, a key feature in the suppression of keratinocyte proliferation. When the organotypic skin was treated with anti-SHH 5E1 monoclonal antibody, the deviations from wild-type epidermis listed above were mitigated, supporting the notion that NBCCS fibroblasts hyper-secrete SHH and disrupt the epidermis by means of the SHH signaling pathway.

An in vitro organotypic skin model of BCC, where fibroblasts were embedded in a Matrigel-collagen matrix, was created using the manual method to understand PATCHED and other pertinent signaling pathways (Rahman 2013). Various types of immortalized human keratinocytes (HaCaT, NEB1, or N/Tert) were then seeded onto the dermis. The keratinocytes were transfected with PTCH1 short hairpin RNA in order to suppress PATCHED and observe the repercussions. Certain experiments employed SMO RNAi meant to knockdown SMO, a protein downstream of PATCHED in the SHH signaling pathway. Importantly, the 3D model did not fully recreate BCC characteristics seen in in vivo behavior. The study led to multiple conclusions: part of PATCHED is expressed in the nucleus, PATCHED suppression promotes nuclear/perinuclear SMO, and the increase in Gli1 due to PATCHED suppression is not significantly responsive to SMO inhibitors. These findings corroborate that SMO-independent mechanisms are likely involved when PTCH1 is knocked down, resulting in the persistent BCC phenotype despite the presence of pharmaceutical treatments targeting SMO.

Hehlgans et al. tested a 3D colony formation assay that provided BCC-1 cells a more epidermis-like environment compared to 2D plating (Hehlgans et al. 2018). The BCC-1 cells were diluted into a laminin-rich extracellular matrix, and certain experiments were treated with vismodegib, a monotherapy drug that inhibits the Hedgehog signaling pathway, as well as radiation. Unlike the 2D models, the 3D experiments demonstrated that vismodegib significantly sensitizes BCC cells to radiation, causing a higher fraction of dead cells as the concentration of vismodegib increases. The fabricated cancer model proved to be useful in observing and assessing pre-clinical outcomes of treatment combinations.

3 Discussion and Conclusion

So far, various advanced skin tissue models have been developed to study cancer research. However, the majority of these studies have included only one layer (epidermis) or two layers (epidermis and dermis), neglecting the hypodermis despite the significant roles of adipocytes and adipose tissue in skin cancer. For instance, adipocytes have activated the Akt (Ser-473 and Thr-450) signaling pathway of melanoma cells, thereby promoting melanoma growth (Kwan et al. 2014). Another studies showed that de-differentiation of adipocytes into fibroblast-like cells has been able to trigger melanoma cell migration by activating the signaling pathway of Wnt5a, β-catenin, and LEF-1 (Zoico et al. 2018). As such, leveraging a fully functionalized tri-layered skin tissue model is essential to better understand the molecular mechanism and the pathology of skin cancer.

In addition to cancer, adipose tissue has significantly affected skin tissue regeneration and wound healing. For example, a novel functional hypodermal-dermo-epidermal tri-layered skin substitute with vascularization was proposed by Zimoch et al. (2021). It was suggested that adipose mesenchymal stem cell-derived adipocytes and TGF-β1 secreted by these cells in adipose tissue had a profound impact on the maturation and differentiation of keratinocytes and fibroblasts as well as epidermal morphogenesis. Monfort et al. also observed a similar effect with hypodermis components that promote epidermal differentiation (i.e., differentiation of epithelial cells into mature keratinocytes) using a tri-layered fibrin-based skin substitute (Monfort et al. 2013).

There are still some limitations to fabricating a functional adipose tissue – in particular, preadipocyte differentiation. It is substantially difficult to induce preadipocyte differentiation in vivo. This is because primary cells have a limited life span. In addition, the isolation of preadipocytes from fibroblast-like cells is another challenge to overcome (Ntambi and Kim 2000). Hence, adipose precursor cell lines such as pluripotent fibroblasts or unipotent preadipocytes have been adopted for the differentiation of preadipocytes into adipocytes due to the stability and unlimited passage as an in vitro model. However, there is still difficulty differentiating preadipocytes into adipocytes due to the susceptibility of adipocytes to in vitro skin tissue, and inconsistent viability by nature (Zimoch et al. 2021). Forming vascular networks in the engineered tissue is also pivotal for cancer modeling. The absence of vascularization in the tissue is known as a major reason for the failure of the transplant of engineered skin tissue (Miyazaki et al. 2019). However, vascularization is a challenging part in the field of tissue engineering (Auger et al. 2013). In particular, replicating simultaneous vascularization and adipogenesis in 3D scaffolds is extremely difficult. Prior studies showed that human microvascular endothelial cells (HMVEC) or human umbilical vein endothelial cells (HUVEC) could be useful for recapitulating a more complex tumor microenvironment with vasculature (Laschke and Menger 2016). Another recent study by Zimoch et al. showed a successful development of prevascularized tri-layered skin substitutes and implanted them in mice for the first time (Zimoch et al. 2021). Moreover, the majority of research using in vitro tumor models has been focused on the interaction between the tumor and its microenvironment, whereas few studies have been performed on understanding a tissue-specific microenvironment (Bourland et al. 2018). In addition to these limitations, understanding tumor heterogeneity in terms of mutations, and selecting appropriate biomaterials and model designs are enormous hurdles to be addressed (Unnikrishnan et al. 2021).

Over the last decades, skin cancer incidence has rapidly increased by repeated and unprotected skin exposure to ultraviolet (UV) rays from sunlight. As such, developing a functional full-thickness tri-layered 3D skin model is needed to predict more accurate cancer cell behavior as well as drug screening and efficacy. Future treatments for skin cancer may be significantly impacted and developed by the use of these 3D cancer models for personalized medicine.

References

Akgül B, García-Escudero R, Ghali L, Pfister HJ, Fuchs PG, Navsaria H, Storey A (2005) The E7 protein of cutaneous human papillomavirus type 8 causes invasion of human keratinocytes into the dermis in organotypic cultures of skin. Cancer Res 65:2216. https://doi.org/10.1158/0008-5472.CAN-04-1952

Asghar W, El Assal R, Shafiee H, Pitteri S, Paulmurugan R, Demirci U (2015) Engineering cancer microenvironments for in vitro 3-D tumor models. Mater Today 18(10):539–553

Auger FA, Gibot L, Lacroix D (2013) The pivotal role of vascularization in tissue engineering. Annu Rev Biomed Eng 15:177. https://doi.org/10.1146/annurev-bioeng-071812-152428

Bernerd F, Asselineau D, Vioux C, Chevallier-Lagente O, Bouadjar B, Sarasin A, Magnaldo T (2001) Clues to epidermal cancer proneness revealed by reconstruction of DNA repair-deficient xeroderma pigmentosum skin in vitro. Proc Natl Acad Sci U S A 98:7817. https://doi.org/10.1073/pnas.141221998

Bigelow RLH, Jen EY, Delehedde M, Chari NS, McDonnell TJ (2005) Sonic hedgehog induces epidermal growth factor dependent matrix infiltration in HaCat keratinocytes. J Invest Dermatol 124:457. https://doi.org/10.1111/j.0022-202X.2004.23590.x

Bouez C, Reynaud C, Noblesse E, Thépot A, Gleyzal C, Kanitakis J, Perrier E, Damour O, Sommer P (2006) The lysyl oxidase LOX is absent in basal and squamous cell carcinomas and its knockdown induces an invading phenotype in a skin equivalent model. Clin Cancer Res 12:1463. https://doi.org/10.1158/1078-0432.CCR-05-1456

Bourland J, Fradette J, Auger FA (2018) Tissue-engineered 3D melanoma model with blood and lymphatic capillaries for drug development. Sci Rep 8. https://doi.org/10.1038/s41598-018-31502-6

Brauchle E, Johannsen H, Nolan S, Thude S, Schenke-Layland K (2013) Design and analysis of a squamous cell carcinoma in vitro model system. Biomaterials 34:7401. https://doi.org/10.1016/j.biomaterials.2013.06.016

Brellier F, Bergoglio V, Valin A, Barnay S, Chevallier-Lagente O, Vielh P, Spatz A, Gorry P, Avril MF, Magnaldo T (2008) Heterozygous mutations in the tumor suppressor gene PATCHED provoke basal cell carcinoma-like features in human organotypic skin cultures. Oncogene 27:6601. https://doi.org/10.1038/onc.2008.260

Browning JR, Derr P, Derr K, Doudican N, Michael S, Lish SR, Taylor NA, Krueger JG, Ferrer M, Carucci JA, Gareau DS (2020) A 3D biofabricated cutaneous squamous cell carcinoma tissue model with multi-channel confocal microscopy imaging biomarkers to quantify antitumor effects of chemotherapeutics in tissue. Oncotarget. https://doi.org/10.18632/oncotarget.27570

Cakir BÖ, Adamson P, Cingi C (2012) Epidemiology and economic burden of nonmelanoma skin cancer. Facial Plast Surg Clin North Am 20(4):419–422

Carvalho MR, Lima D, Reis RL, Correlo VM, Oliveira JM (2015) Evaluating biomaterial- and microfluidic-based 3D tumor models. Trends Biotechnol 33(11):667–678

Carvalho MR, Reis RL, Oliveira JM (2018) Mimicking the 3D biology of osteochondral tissue with microfluidic-based solutions: breakthroughs towards boosting drug testing and discovery. Drug Discov Today 23(3):711–718

Cui X, Hartanto Y, Zhang H (2017) Advances in multicellular spheroids formation. J R Soc Interface 14(127):20160877

Dahmane N, Lee J, Robins P, Heller P, Ruiz I, Altaba A (1997) Activation of the transcription factor Gli1 and the sonic hedgehog signalling pathway in skin tumours. Nature 389:876. https://doi.org/10.1038/39918

Derr K, Zou J, Luo K, Song MJ, Sittampalam GS, Zhou C, Michael S, Ferrer M, Derr P (2019) Fully three-dimensional bioprinted skin equivalent constructs with validated morphology and barrier function. Tissue Eng Part C Methods 25:334. https://doi.org/10.1089/ten.tec.2018.0318

Di Blasio S, van Wigcheren GF, Becker A, van Duffelen A, Gorris M, Verrijp K, Stefanini I, Bakker GJ, Bloemendal M, Halilovic A, Vasaturo A, Bakdash G, Hato SV, de Wilt JHW, Schalkwijk J, de Vries IJM, Textor JC, van den Bogaard EH, Tazzari M, Figdor CG (2020) The tumour microenvironment shapes dendritic cell plasticity in a human organotypic melanoma culture. Nat Commun 11. https://doi.org/10.1038/s41467-020-16583-0

Dubas LE, Ingraffea A (2013) Nonmelanoma skin cancer. J Cutan Aesthet Surg 5(1):3–10

Duval K, Grover H, Han LH, Mou Y, Pegoraro AF, Fredberg J, Chen Z (2017) Modeling physiological events in 2D vs. 3D cell culture. Physiology (Bethesda) 32(4):266–277

Engelmann L, Thierauf J, Laureano NK, Stark HJ, Prigge ES, Horn D, Freier K, Grabe N, Rong C, Federspil P, Zaoui K, Plinkert PK, Rotter N, von Doeberitz MK, Hess J, Affolter A (2020) Organotypic co-cultures as a novel 3D model for head and neck squamous cell carcinoma. Cancers (Basel). https://doi.org/10.3390/cancers12082330

Gache Y, Brellier F, Rouanet S, Al-Qaraghuli S, Goncalves-Maia M, Burty-Valin E, Barnay S, Scarzello S, Ruat M, Sevenet N, Avril MF, Magnaldo T (2015) Basal cell carcinoma in Gorlin's patients: a matter of fibroblasts-led protumoral microenvironment? PLoS One 10. https://doi.org/10.1371/journal.pone.0145369

Gonçalves-Maia M, Gache Y, Basante M, Cosson E, Salavagione E, Muller M, Bernerd F, Avril MF, Schaub S, Sarasin A, Braud VM, Magnaldo T (2020) NK cell and fibroblast-mediated regulation of skin squamous cell carcinoma invasion by CLEC2A is compromised in xeroderma pigmentosum. J Invest Dermatol 140:1723. https://doi.org/10.1016/j.jid.2020.01.021

Gutschalk CM, Herold-Mende CC, Fusenig NE, Mueller MM (2006) Granulocyte colony-stimulating factor and granulocyte-macrophage colony-stimulating factor promote malignant growth of cells from head and neck squamous cell carcinomas in vivo. Cancer Res 66:8026. https://doi.org/10.1158/0008-5472.CAN-06-0158

Haridas P, McGovern JA, McElwain SDL, Simpson MJ (2017) Quantitative comparison of the spreading and invasion of radial growth phase and metastatic melanoma cells in a three-dimensional human skin equivalent model. PeerJ 5:e3754. https://doi.org/10.7717/peerj.3754

Hehlgans S, Booms P, Güllülü Ö, Sader R, Rödel C, Balermpas P, Rödel F, Ghanaati S (2018) Radiation sensitization of basal cell and head and neck squamous cell carcinoma by the hedgehog pathway inhibitor vismodegib. Int J Mol Sci 19. https://doi.org/10.3390/ijms19092485

Jensen C, Teng Y (2020) Is it time to start transitioning from 2D to 3D cell culture? Front Mol Biosci 7:33

Khavari PA (2006) Modelling cancer in human skin tissue. Nat Rev Cancer 6(4):270–280

Kuzu OF, Nguyen FD, Noory MA, Sharma A (2015) Current state of animal (mouse) modeling in melanoma research. Cancer Growth Metastasis 8s1:CGM.S21214. https://doi.org/10.4137/cgm.s21214

Kwan HY, Fu X, Liu B, Chao X, Chan CL, Cao H, Su T, Tse AKW, Fong WF, Yu ZL (2014) Subcutaneous adipocytes promote melanoma cell growth by activating the Akt signaling pathway: role of palmitic acid. J Biol Chem 289:30525. https://doi.org/10.1074/jbc.M114.593210

Laschke MW, Menger MD (2016) Prevascularization in tissue engineering: current concepts and future directions. Biotechnol Adv 34(2):112–121

Lee JT, Li L, Brafford PA, Van Den Eijnden M, Halloran MB, Sproesser K, Haass NK, Smalley KSM, Tsai J, Bollag G, Herlyn M (2010) PLX4032, a potent inhibitor of the B-Raf V600E oncogene, selectively inhibits V600E-positive melanomas. Pigment Cell Melanoma Res 23:820. https://doi.org/10.1111/j.1755-148X.2010.00763.x

Lelièvre SA, Kwok T, Chittiboyina S (2017) Architecture in 3D cell culture: an essential feature for in vitro toxicology. Toxicol Vitr 45:287. https://doi.org/10.1016/j.tiv.2017.03.012

Li W, Hu X, Yang S, Wang S, Zhang C, Wang H, Cheng YY, Wang Y, Liu T, Song K (2019) A novel tissue-engineered 3D tumor model for anti-cancer drug discovery. Biofabrication 11. https://doi.org/10.1088/1758-5090/aae270

Mak IWY, Evaniew N, Ghert M (2014) Lost in translation: animal models and clinical trials in cancer treatment. Am J Transl Res 6(2):114–118

Marques CMDG, MacNeil S (2016) Use of a tissue engineered human skin model to investigate the effects of wounding and of an anti-inflammatory on melanoma cell invasion. PLoS One 11. https://doi.org/10.1371/journal.pone.0156931

Marsh D, Dickinson S, Neill GW, Marshall JF, Hart IR, Thomas GJ (2008) αvβ6 integrin promotes the invasion of morphoeic basal cell carcinoma through stromal modulation. Cancer Res. https://doi.org/10.1158/0008-5472.CAN-08-0174

Meier F, Nesbit M, Hsu MY, Martin B, Van Belle P, Elder DE, Schaumburg-Lever G, Garbe C, Walz TM, Donatien P, Crombleholme TM, Herlyn M (2000) Human melanoma progression in skin reconstructs: biological significance of bFGF. Am J Pathol 156:193. https://doi.org/10.1016/S0002-9440(10)64719-0

Meier F, Busch S, Lasithiotakis K, Kulms D, Garbe C, Maczey E, Herlyn M, Schittek B (2007) Combined targeting of MAPK and AKT signalling pathways is a promising strategy for melanoma treatment. Br J Dermatol 156:1204. https://doi.org/10.1111/j.1365-2133.2007.07821.x

Mittapalli VR, Madl J, Löffek S, Kiritsi D, Kern JS, Römer W, Nyström A, Bruckner-Tuderman L (2016) Injury-driven stiffening of the dermis expedites skin carcinoma progression. Cancer Res 76:940. https://doi.org/10.1158/0008-5472.CAN-15-1348

Miyazaki H, Tsunoi Y, Akagi T, Sato S, Akashi M, Saitoh D (2019) A novel strategy to engineer pre-vascularized 3-dimensional skin substitutes to achieve efficient, functional engraftment. Sci Rep 9. https://doi.org/10.1038/s41598-019-44113-6

Monfort A, Soriano-Navarro M, García-Verdugo JM, Izeta A (2013) Production of human tissue-engineered skin trilayer on a plasma-based hypodermis. J Tissue Eng Regen Med 7:479. https://doi.org/10.1002/term.548

Ntambi JM, Kim YC (2000) Adipocyte differentiation and gene expression. J Nutr 130(12):3122S–3126S

Obrigkeit DH, Jugert FK, Beermann T, Baron JM, Frank J, Merk HF, Bickers DR, Abuzahra F (2009) Effects of photodynamic therapy evaluated in a novel three-dimensional squamous cell carcinoma organ construct of the skin. Photochem Photobiol 85:272. https://doi.org/10.1111/j.1751-1097.2008.00432.x

Park S, Seawright A, Park S, Dutton JC, Grinnell F, Han B (2015) Preservation of tissue microstructure and functionality during freezing by modulation of cytoskeletal structure. J Mech Behav Biomed Mater 45:32. https://doi.org/10.1016/j.jmbbm.2015.01.014

Rahman MM (2013) Characterisation of a novel in vitro model of basal cell carcinoma (BCC) through stable PTCH1 suppression in immortalised human keratinocytes. Theses. Queen Mary University of London

Smirnov A, Lena AM, Cappello A, Panatta E, Anemona L, Bischetti S, Annicchiarico-Petruzzelli M, Mauriello A, Melino G, Candi E (2019) ZNF185 is a p63 target gene critical for epidermal differentiation and squamous cell carcinoma development. Oncogene 38:1625. https://doi.org/10.1038/s41388-018-0509-4

Syed DN, Chamcheu JC, Khan MI, Sechi M, Lall RK, Adhami VM, Mukhtar H (2014) Fisetin inhibits human melanoma cell growth through direct binding to p70S6K and mTOR: findings from 3-D melanoma skin equivalents and computational modeling. Biochem Pharmacol 89:349. https://doi.org/10.1016/j.bcp.2014.03.007

Unnikrishnan K, Thomas LV, Ram Kumar RM (2021) Advancement of scaffold-based 3D cellular models in cancer tissue engineering: an update. Front Oncol 11:733652

Van Kilsdonk JWJ, Bergers M, Van Kempen LCLT, Schalkwijk J, Swart GWM (2010) Keratinocytes drive melanoma invasion in a reconstructed skin model. Melanoma Res 20:372. https://doi.org/10.1097/CMR.0b013e32833d8d70

Vörsmann H, Groeber F, Walles H, Busch S, Beissert S, Walczak H, Kulms D (2013) Development of a human three-dimensional organotypic skin-melanoma spheroid model for in vitro drug testing. Cell Death Dis 4. https://doi.org/10.1038/cddis.2013.249

Zarebkohan A, Sheervalilou R, Ghods R, Kundu SC, Gholipourmalekabadi M (2020) 3D scaffold materials for skin cancer modeling. In: Biomaterials for 3D tumor modeling. https://doi.org/10.1016/B978-0-12-818128-7.00014-9

Zimoch J, Zielinska D, Michalak-Micka K, Rütsche D, Böni R, Biedermann T, Klar AS (2021) Bio-engineering a prevascularized human tri-layered skin substitute containing a hypodermis. Acta Biomater 134:215. https://doi.org/10.1016/j.actbio.2021.07.033

Zoico E, Darra E, Rizzatti V, Tebon M, Franceschetti G, Mazzali G, Rossi AP, Fantin F, Zamboni M (2018) Role of adipose tissue in melanoma cancer microenvironment and progression. Int J Obes 42:344. https://doi.org/10.1038/ijo.2017.218

Zoschke C, Ulrich M, Sochorová M, Wolff C, Vávrová K, Ma N, Ulrich C, Brandner JM, Schäfer-Korting M (2016) The barrier function of organotypic non-melanoma skin cancer models. J Control Release 233:10. https://doi.org/10.1016/j.jconrel.2016.04.037